Improving the extension–twist coupling performance of practically warpage-free laminates via layup hybridization

Vermes B., Czigány T.

Accepted for publication in Journal of Reinforced Plastics and Composites
Published in 2023
DOI: 10.1177/07316844221102941

Improving the extension–twist coupling performance of practically warpage-free laminates via layup hybridization

Bruno Vermes[1,2], Tibor Czigany[1,2]*

[1] Department of Polymer Engineering, Faculty of Mechanical Engineering, Budapest University of Technology and Economics, Műegyetem rkp. 3., H-1111 Budapest, Hungary

[2] MTA-BME Research Group for Composite Science and Technology, Műegyetem rkp. 3., H-1111 Budapest, Hungary

* corresponding author: czigany@eik.bme.hu

Abstract

This article investigates whether the extension–twist and bend–twist coupling performance of practically warpage-free laminates can be improved by layup hybridization (carbon/epoxy-glass/epoxy hybrids) compared to non-hybrid (mono) laminates. We performed numerical layup search by simulating the thermal warpage, and the bend–twist and extension–twist behaviour of 4096 4-ply layup permutations. The upper limit of allowable manufacturing induced warpage was based on the ISO2768 standard. The optimal hybrid and mono layups were selected to have the most significant coupling performance within the allowable warpage range. A mono layup achieved the maximum bend–twist performance (which does not require layup asymmetry), but layup hybridization increased the extension–twist performance by more than 30% in the practically warpage-free range. The numerical results were validated through 3D scanning and 3D digital image correlation–aided mechanical tests. We concluded that layup hybridization can significantly improve the extension–twist performance of realistically usable composite laminates with negligible thermal warpage.

Keywords: Hybrid composites, morphing laminates, asymmetric layup, numerical analysis, experimental validation

1. Introduction

Composites have proven to be one of the most valuable structural materials, primarily due to their excellent specific mechanical properties, but their value can be further increased by making them multifunctional. The additional functionality can be anything from self-healing [1–3] to self-sensing [4], shape-memory [5] and beyond. However, the most fundamental extra feature of composites might be their intrinsic coupled mechanical behaviour which results from their layup structure and makes them suitable for morphing applications. Bend–twist [6,7] and extension–twist [8] laminates are especially valuable because of their industrial significance as advanced turbine blade materials, for instance. However, the majority of coupled laminates have asymmetric layups causing limited usability due to warpage. Although not all asymmetric laminates warp, hygrothermally stable ones are relatively rare [9]. Asymmetric laminates can also be bistable, which further complicates the mitigation of their warpage. Monostable laminates have one stable shape that looks like a saddle because both principal curvatures of the laminate are significant. Bistable laminates have two stable cylindrical shapes - with only one significant principal curvature per shape -, which can be converted into each other via a snap-through effect. The monostable and bistable regions are separated by the bifurcation point, which is affected by the material properties and the layup structure of the laminate. For laminates with given material properties and layup structure, monostability can be ensured with a large

enough relative thickness that reduces the edge-length to thickness ratio below the bifurcation point of the specific layup [10,11].

Mitigating manufacturing-induced distortions, such as the spring-in effect [12], have always been one of the main challenges in the composites industry. Tool compensation methods are among the most widespread techniques to tackle the issue. These methods take the manufacturing-induced distortions (e.g. thermal warpage) of the laminate into account by modifying the dimensions of the manufacturing tool. For instance, if the desired nominal shape of the composite part should include a 90° corner, the manufacturing tool has to be designed with a larger than 90° corner to compensate for the spring-in effect [13]. Similarly, it is possible to compensate for the warpage of asymmetric laminates with the geometry of the tool. From a mechanical coupling standpoint, the advantage of the method is that it does not modify the layup, which would potentially reduce the coupling performance of the laminate. On the other hand, the shape of the laminate remains temperature-dependent, which can be a major limitation of the method.

Layup homogenization is another effective method to mitigate warpage. However, placing a number of identical sub-laminates on top of each other reduces the layup asymmetry–dependent coupling performance, too [14].

Hygrothermally stable laminates solve the issue of warpage with clever layup designs while retaining some of the desired coupling performance of the laminate – e.g. hygrothermally stable extension–twist laminates [15]. There are two necessary and sufficient conditions for hygrothermal stability. The first condition is a zero extensional-bending coupling compliance matrix (*[b]*) based on the classical laminate theory (Eq. (1)), which is automatically satisfied by symmetric laminates but can also be satisfied by asymmetric laminates in rare instances. Unfortunately, this also rules out any extension–twist coupling, for instance. The second set of conditions requires the first two in-plane non-mechanical stress resultants to be equal and all other non-mechanical stress resultants to be zero. This second condition can finally be satisfied by asymmetric extension–twist laminates with a non-zero *[b]* matrix [9,16]. The main issue with the hygrothermally stable laminate concept is that only very specific layups fulfil the necessary and sufficient conditions, which greatly limits the potentially achievable coupling performance. Equation (1) illustrates the constitutive matrix equation of the classical laminate theory, where ε^0 is the mid-plane strain κ is the curvature, *N* and *M* are the in-plane and out-of plane stress resultants (loads and moments per unit width), *[a]* is the extensional compliance matrix, *[b]* is the extensional-bending coupling compliance matrix, *[d]* is the bending compliance matrix and *x*, *y* and *z* are the longitudinal and transverse in-plane and the through-thickness out-of-plane structural coordinates of the laminate, respectively [17]:

$$\begin{bmatrix} \varepsilon^0{}_{xx} \\ \varepsilon^0{}_{yy} \\ \varepsilon^0{}_{xy} \\ \kappa_{xx} \\ \kappa_{yy} \\ \kappa_{xy} \end{bmatrix} = \begin{bmatrix} a_{11} & a_{12} & a_{16} & b_{11} & b_{12} & b_{16} \\ a_{12} & a_{22} & a_{26} & b_{21} & b_{22} & b_{26} \\ a_{16} & a_{26} & a_{66} & b_{61} & b_{62} & b_{66} \\ b_{11} & b_{21} & b_{61} & d_{11} & d_{12} & d_{16} \\ b_{12} & b_{22} & b_{62} & d_{12} & d_{22} & d_{26} \\ b_{16} & b_{26} & b_{66} & d_{16} & d_{26} & d_{66} \end{bmatrix} \begin{bmatrix} N_{xx} \\ N_{yy} \\ N_{xy} \\ M_{xx} \\ M_{yy} \\ M_{xy} \end{bmatrix} \quad (1)$$

When it comes to minimizing the thermal warpage and maximizing the desired coupling (e.g. extension–twist) performance of composites, hybrid layups could offer a better trade-off than other methods. Layups can be hybridized in many ways, but it is most commonly done by combining two (or

more) kinds of plies with different fibre reinforcements (e.g. carbon/epoxy–glass/epoxy hybrids). Hybridization has been shown to be advantageous in many applications, including pseudo-ductile [18] and high damping [19] laminates, shape memory alloy composites [20], laminates with built-in overload sensors [21] or adaptive multistable structures with advanced mechanical performance [22]. The advanced behaviour of the hybrid laminate results from the complex effects of combining plies with different mechanical, thermal, etc. properties, but hybridization also increases the number of layup permutations significantly, which promotes finding a better performing laminate. The main question that needs to be answered is whether the complex effects of hybridization can improve the desired coupling performance compared to non-hybrid laminates while still ensuring a practically warpage-free manufacturing process for real-world usability.

Therefore, this paper aims to investigate whether layup hybridization is a feasible method to improve the bend–twist or the extension–twist coupling performance of practically thermal warpage-free laminates (based on the ISO2768 standard). First, we experimentally determine the edge-length to thickness ratio of the laminate where we can analyze all mono and hybrid layups in their monostable state to avoid potential simulation inaccuracies resulting from bistability. This is necessary for drawing well-founded conclusions from the simulation results as preliminary comparison of experimental and simulation results showed that the latter did not always capture bistablity reliably. Then, we carry out a full-field numerical study to quantify and compare the thermal warpage, and the bend–twist and extension–twist performance of mono and hybrid layups. And finally, before drawing conclusions, we validate the numerical results by experimentally investigating the best-performing layups from each layup family (carbon mono, glass mono and carbon/glass hybrid).

2. Materials and methods

To investigate the potential advantages of layup hybridization, we used unidirectional carbon/epoxy and glass/epoxy prepregs and utilized analytical, numerical and experimental methods.

2.1. Materials

We used two kinds of prepreg materials to investigate mono and hybrid laminates. The Hexcel IM7/913 carbon–epoxy unidirectional (UD) and the Hexcel S-Glass/913 glass–epoxy UD prepregs featured the same matrix material, which prevented quality issues that could arise from matrix mismatch. Table 1 contains the relevant properties of the two prepregs. The longitudinal (E_1), transverse (E_2) and shear (G_{12}) moduli, as well as the in-plane Poisson's ratio (ν_{12}), were either obtained from the manufacturer or calculated from the properties of the individual components with the use of the rule of mixtures, while the thickness of the cured plies and the thermal expansion coefficients (longitudinal α_0 and transverse α_{90}) were measured [23,24]. Thermal expansion tests were carried out in a calibrated heating chamber in the 25 °C to 140 °C temperature range. We used KMT-LIAS-06-1,5-350-5E strain gauges in the longitudinal and transverse directions bonded on autoclave manufactured (140 °C, 7 bar) 50 mm x 50 mm 4-ply UD laminates using Vishay M-Bond 610 adhesive. Strain data was gathered with an HBM Spider8 general data acquisition device, and we also carried out baseline tests on a piece of quartz glass with a known and extremely low thermal expansion to eliminate any inaccuracies arising from the temperature dependence of the gauges. The accuracy of the results was validated by comparing numerically and experimentally (3D scanning) obtained thermal warpage data of a number of different glass–epoxy and carbon–epoxy layups.

Table 1. Relevant properties of the carbon–epoxy and the glass–epoxy prepregs

Reinforcement	HexTow IM7 UD carbon	Hexcel UD S-Glass
Matrix	HexPly 913 epoxy	HexPly 913 epoxy
E_1 (GPa)	163.30	45.70
E_2 (GPa)	8.74	6.41
G_{12} (GPa)	4.50	2.75
ν_{12} (-)	0.30	0.27
α_0 ($°C^{-1}$)	3.00 x 10^{-7}	8.10 x 10^{-6}
α_{90} ($°C^{-1}$)	3.20 x 10^{-5}	3.60 x 10^{-5}
Cured ply thickness (mm)	0.13	0.15

2.2. Analytical method

As a preliminary study, we used a self-developed classical laminate theory (CLT) based MATLAB algorithm to find the carbon–epoxy and glass–epoxy mono layups with the most significant thermal warpage. The reason for this was to later find a laminate edge-length to thickness ratio where all mono and hybrid layups were expected to behave monostable to avoid complications arising from bistability. Thermal loads were calculated according to [25], from the difference between the autoclave plateau temperature and the room temperature ΔT=115 °C (see 2.4.1.) using Eqs. (2) and (3). In the equations N_x^T, N_y^T and N_{xy}^T refer to the thermal forces per unit length, M_x^T, M_y^T and M_{xy}^T are the thermal moments per unit length, ΔT is the change in temperature (°C), k is the ordinal number of the ply in the layup, $[\bar{Q}]$ is the stiffness matrix of the ply in the structural direction, α_x, α_y and α_{xy} are the in-plane thermal coefficients of the ply in the structural direction (there are only two in the material direction), t_k is the thickness of the ply and $\bar{z}_k$ is the distance of the ply mid-plane from the laminate mid-plane. In Eq. (1), the mechanical loads can be replaced with the thermal loads when only thermal loading is present.

$$\begin{bmatrix} N_x^T \\ N_y^T \\ N_{xy}^T \end{bmatrix} = \Delta T \sum_{k=1}^{N} [\bar{Q}]^k \begin{bmatrix} \alpha_x \\ \alpha_y \\ \alpha_{xy} \end{bmatrix}^k t_k \tag{2}$$

$$\begin{bmatrix} M_x^T \\ M_y^T \\ M_{xy}^T \end{bmatrix} = -\Delta T \sum_{k=1}^{N} [\bar{Q}]^k \begin{bmatrix} \alpha_x \\ \alpha_y \\ \alpha_{xy} \end{bmatrix}^k t_k \bar{z}_k \tag{3}$$

More than 20,000 layup permutations were analyzed for both materials during the full-field investigation of 4-ply 100 mm x 100 mm laminates with an orientation increment of 15°. Warpage was quantified by the height of the encasing cuboid of the deformed laminate. The previously introduced analytical solution of CLT has limited accuracy and always predicts saddle shapes, but we took the cylindrical bistable shapes into account in subsequent experiments. The main goal of the analytical layup search was not to obtain accurate deformations but to find the potentially most significantly warping carbon–epoxy and glass–epoxy layups so that we could investigate them further experimentally (see 2.4. and 3.1.). Based on the CLT calculations, the extent of warpage depends on the ply-thickness, but the layup

structure of the maximally warping laminate does not. This is important, as later numerical and experimental investigations were carried out on laminates with triple the thickness (see 2.3. and 2.4.).

2.3. Numerical methods

The thermal warpage and the bend–twist and extension–twist performances of the mono and hybrid laminates were simulated in ANSYS Workbench 2019 R3 (Composites PrepPost extension). We investigated 40 mm x 40 mm laminates with theoretically 4, but actually 12 plies as each ply had 3 times the thickness of that in Table 1 (i.e. 0.39 mm thick carbon–epoxy and 0.45 mm thick glass–epoxy plies). The reason for this was to avoid complications resulting from bistability (see the results in 3.1.).

As numerical calculations are significantly slower than analytical calculations, we increased the orientation increment of the plies to 45° to decrease the number of layup permutations. This way, each ply in the laminate could be placed in either of the four industry-standard fibre orientations: 0°, 45°, -45° and 90°. After building the numerical models and running the mesh convergence studies, we ran the three types of simulations for all 4096 layup permutations (512 mono and 3584 hybrid layups).

For the warpage and the bend–twist simulations, shell elements were used as solid simulations would have taken significantly longer to solve and shell and solid results differed less than 1% even at large deformations during our preliminary trials. On the other hand, for the extension–twist simulations we used solid elements instead of shell elements because we found that results with the two types of elements differed by more than 3% and solid elements approximated experimental results better. The first set of simulations was run for thermal warpage with the following parameters: square SHELL181 elements (four-node element with six degrees of freedom at each node – three translational and three rotational) with 1 mm edge-length, laminate fixed at its mid-point, thermal load ΔT=115 °C (cool-down from the autoclave plateau temperature of 140 °C to room temperature 25 °C) and large deflections enabled (i.e. calculating with geometrical nonlinearity). Warpage was quantified by the height of the encasing cuboid of the warped laminate. Ansys provided the out-of-plane (z-direction) displacements of each point of the laminate as a result of thermal loading, and the difference between the maximum and the minimum values gave the height of the encasing cuboid. The second set of simulations solved for twisting under bending load with the following parameters: square SHELL181 elements (four-node element with six degrees of freedom at each node – three translational and three rotational) with 1 mm edge-length, laminate fixed along one of its edges (along x) and out-of-plane displacement applied at a circular area with a 2 mm radius at the middle of its opposite edge (meshing of the circular area and its close proximity was done automatically by Ansys based on the globally set 1 mm edge length), with large deflections enabled. From the results, we calculated the torsional angle of the loaded edge from the coordinates of its two endpoints at 5 mm of its midpoint deflection. The last set of simulations also investigated the twisting deformation of the laminate, but instead of a bending load, the specimens were subjected to a tensile load. The extension–twist simulations were carried out similarly to the bend–twist simulations, but with cuboid SOLID185 elements (eight-node element with three translational degrees of freedom at each node) with 1 mm edge-length in the plane of the laminate and applied in-plane displacement of the loaded edge (free movement of the edge otherwise). Torsion was calculated at 0.5% (0.2 mm) longitudinal in-plane strain. We specified the displacement of the loaded edge instead of the applied force mainly to avoid aborted simulations due to the order of magnitude

differences in the directional stiffness of different laminates (e.g. laminates with only longitudinal reinforcement vs. laminates with only transverse reinforcement). In each case, the global torsion of the loaded edge was calculated from the out-of-plane (z-direction) coordinates of the two corner points of the edge according to Eq. (4), where α is the global rotational angle of the loaded edge, L is the length of the loaded edge ($L = 40\ mm$) and z_1 and z_2 are the z coordinates (in mm) of the two corner points of the loaded edge Torsion was calculated at 5 mm mid-point deflection for the bend-twist laminates and at 0.5% strain for the extension-twist laminates. The absolute value of the torsional angle was calculated to better compare the magnitude of the achievable twisting performance of the laminates.

$$|\alpha| = arcsin\frac{|z_1 - z_2|}{L} \tag{4}$$

2.4. Experimental methods

We subjected mono and hybrid laminates to 3D scanning tests to evaluate their warped shape, and 3D digital image correlation (3D DIC) aided mechanical tests to assess their coupling performance.

2.4.1. Specimen manufacturing

All specimens were manufactured on a flat aluminium tool in an autoclave with the use of the curing cycle illustrated in Figure 1. The cured laminates were cut to the exact specimen dimensions with a Mutronic Diadisc 4200 precision cut-off saw with a diamond cutting disc.

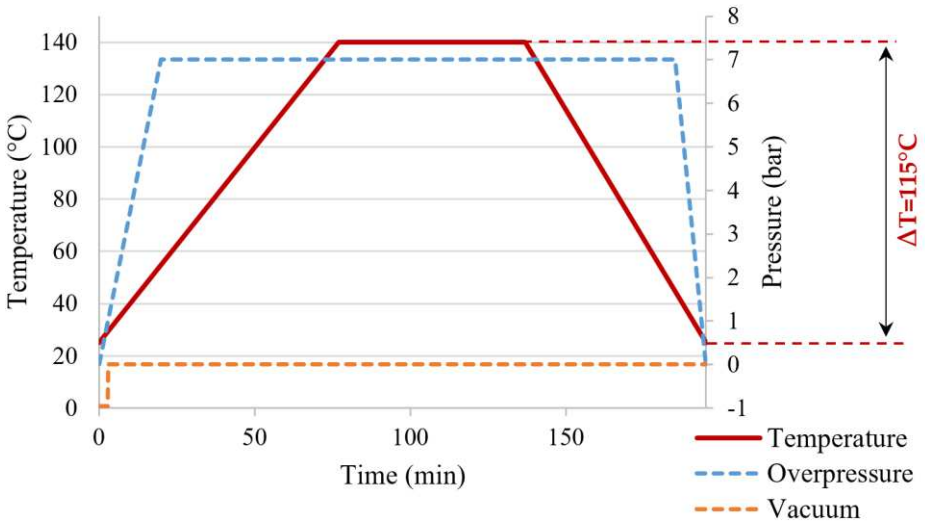

Figure 1 The programmed autoclave curing cycle for specimen manufacturing

2.4.2. 3D scanning evaluation of thermal warpage

To analyse the shape of the warped laminates at room temperature (25 °C), we used a GOM (Gesellschaft für Optische Messtechnik GmbH) ATOS 5M 3D scanner with its ATOS Professional 2018 software. The raw data was evaluated in MATLAB by fitting a second-degree polynomial equation with two variables ($z = ax^2 + bxy + cy^2$) to the scanned points and calculating the height of the encasing cuboid of the deformed specimen and the principal curvatures at the midpoint of the laminate. The coefficient of determination (R^2) of the fitted surface was greater than 0.95 in every case.

We repeated the 3D scanning process of the analytically selected 190 mm x 190 mm carbon–epoxy and glass–epoxy laminates every time after 5 mm was cut off from each of their edges to decrease the edge-

length to thickness ratio, to find their monostable range (details in 3.1.). 3D scanning tests on 40 mm x 40 mm mono and hybrid laminates were also carried out to validate the numerically obtained thermal warpage results (details in 3.3.).

2.4.3. Mechanical tests of coupling performance

The extension–twist mechanical tests were carried out with a hydraulic Instron 8872 universal testing machine with freely rotating grips (0.5 mm/min grip separation). To accurately record the 3D deformation of the specimens under tension, we used a two-camera DIC system (Mercury BFLY 050), which provided 3D strain maps by following the fine sprayed black and white pattern on the specimens' surface (at a sampling rate of 10 Hz). Figure 2 illustrates an example of the 3D DIC results. The DIC system provided high-resolution in-plane and out-of-plane displacement maps of the tensile loaded specimens, so we were able to calculate the torsion of the loaded edge similar to the numerical results. Similarly to the 3D scanning experiments, the DIC–monitored area of the mechanically tested specimens were 40 mm x 40 mm. However, an extra 50 mm length was provided on both sides of the laminates (40 mm for the grip and 10 mm for moving the DIC–monitored area further from the grip), making the dimensions of the specimen 40 mm x 140 mm.

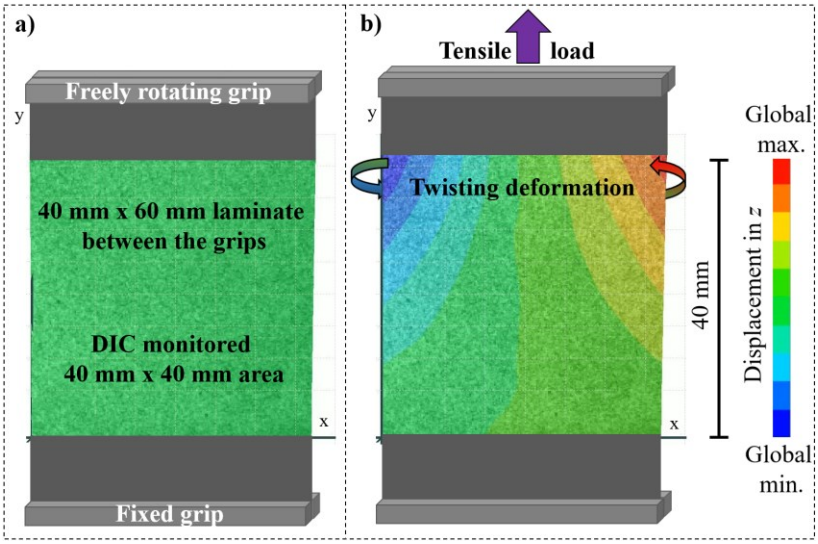

Figure 2 Experimental 3D digital image correlation results of one of the extension–twist hybrid laminates, where colours represent out-of-plane displacement. a) a practically warpage-free specimen gripped along its opposite edges, b) a twisting specimen under an applied tensile load

3. Results and discussion

3.1. Monostable laminate behaviour

The [45/90/-75/-45] carbon–epoxy and the [30/60/-60/-30] glass–epoxy laminates demonstrated the largest thermal warpage based on the full-field analytical layup search. For the 3D scanning experiments, the ply thicknesses were tripled (i.e. 0.39 mm thick carbon–epoxy and 0.45 mm thick glass–epoxy plies) to allow us to reach lower edge-length to thickness ratios, so we manufactured and investigated [45_3 /90_3 /-75_3 /-45_3] carbon–epoxy and [30_3 /60_3 /-60_3 /-30_3] glass–epoxy specimens. Figure 3 illustrates the results of the 3D scanning tests.

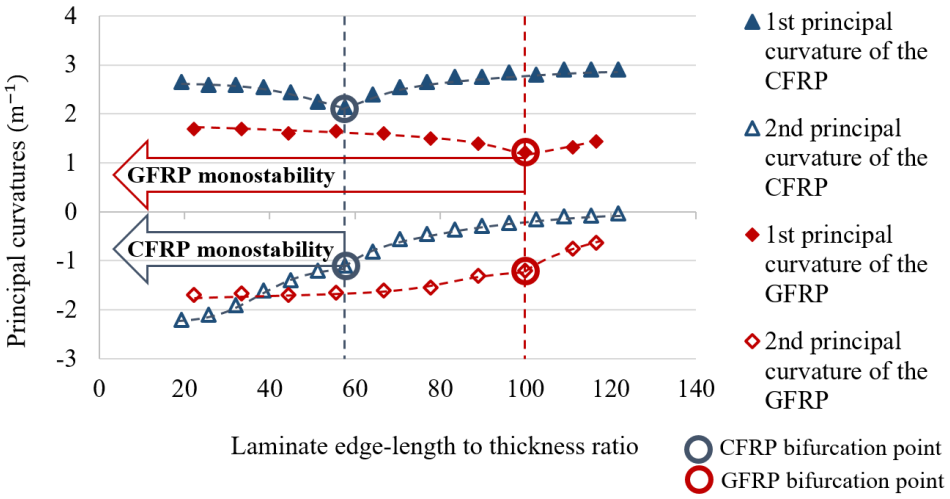

Figure 3 Monostable-bistable transition of the [45_3/90_3/-75_3/-45_3] carbon fibre–reinforced laminate (CFRP) and the [30_3/60_3/-60_3/-30_3] glass fibre–reinforced laminate (GFRP)

The local minimum of the first principal curvature and the significant change in the gradient of the second principal curvature as a function of the edge-length to thickness ratio indicated the bifurcation points of the laminates. The bifurcation point of the carbon–epoxy laminate was identified at a dimensional ratio of around 60 and at around 100 for the glass–epoxy laminate. At lower dimensional ratios, the laminates were monostable. Based on the results, we chose 40 mm x 40 mm 12-ply (4x3 plies) thick laminates for further experiments, which meant a dimensional ratio of 22 for the glass–epoxy laminates and 26 for the carbon–epoxy laminates. The dimensions and the number of plies in the laminate were chosen to be far from bistability, without the small size of the specimens causing any issues during the subsequent 3D scanning and mechanical experiments. The safe distance from the bifurcation point was also meant to ensure that not only the mono laminates but also all the hybrid layups stay within the monostable region.

The stability analysis was necessary because we found that the numerical simulation of the bistable behaviour of laminates was not always accurate during preliminary investigations. Therefore, it was best to avoid bistability to minimize numerical errors and draw valid conclusions on the advantages of layup hybridization.

3.2. Bend–twist coupled laminates

Figure 4 illustrates the thermal warpage and the bend–twist results of the mono and hybrid layups. Based on the ISO 2768-40L standard, any laminate below the dashed red line (0.4 mm encasing cuboid height) was practically warpage-free. The laminates above the limit of flatness were disqualified due to too large deformation, but laminates under the limit were not differentiated based on the magnitude of their warpage, only based on their twisting deformation under bending load. Therefore, the best laminate was the one with the most significant twisting deformation that was still under the limit of flatness. Based on the numerical results, the optimal layup for the combined criteria was a symmetric, full carbon laminate ([45_3 /90_3 /90_3 /45_3]) with no warpage at all. The explanation is that bend–twist coupling does not require layup asymmetry because it is mainly driven by the d_{16} coupling term (which connects M_{xx} with κ_{xy} based on Eq. (1)). Therefore, the warpage mitigating capability of layup hybridization could not be fully exploited in this case.

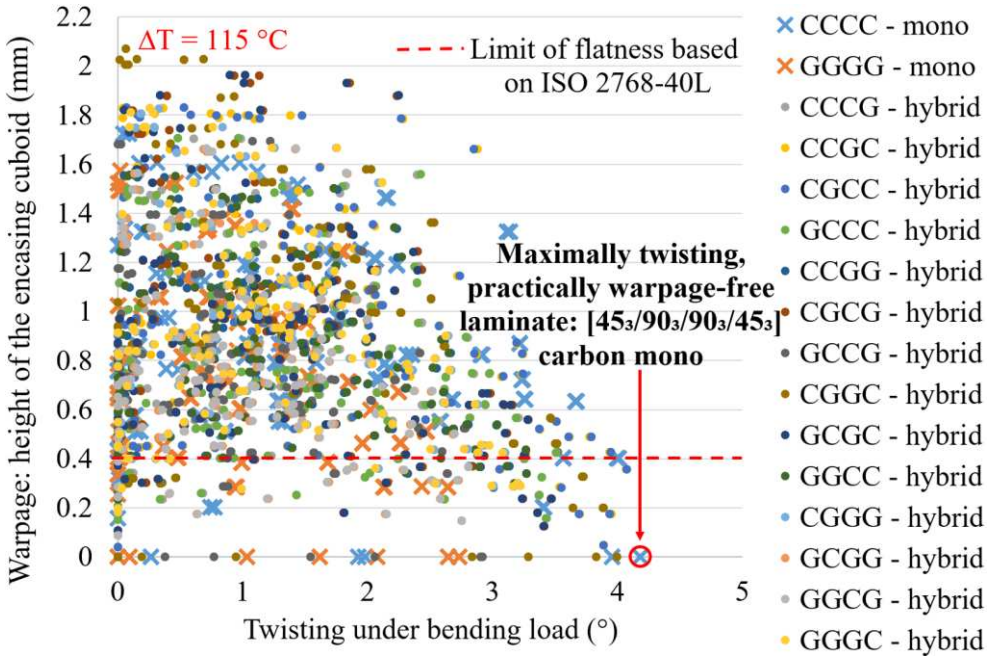

Figure 4 Numerical results for the 40 mm x 40 mm 12-ply (4 x 3 plies) mono and hybrid laminates: warpage at ΔT=115 °C and twisting at 5 mm mid-point deflection of the bending loaded edge, where C refers to carbon and G refers to glass reinforcement

3.3. Extension–twist coupled laminates

Extension–twist laminates are asymmetric, so we were able to investigate the real advantages of hybrid layups on them. Figure 5 illustrates the thermal warpage and the extension–twist results of all the mono and hybrid layups. The selection process was similar to the previous study: the optimal layup was below the dashed red line (limit of flatness) and with the most significant twisting deformation—but now under tension instead of a bending load. The best performing layup was the hybrid [-45_3 /45_3 /90_3 /-45_3] carbon/glass/carbon/carbon laminate. The best hybrid laminate outperformed the best glass mono laminate ([45_3 /-45_3 /45_3 /90_3]) by an impressive 43.5% and the best carbon mono laminate ([45_3 /-45_3 /45_3 /-45_3]) by 59.9% in terms of twisting under tension in the practically warpage-free range. Based on the numerical results, the best hybrid laminate twisted 1.26° at 0.5% strain, which is a significant amount considering that the specimen was only 40 mm long. Over greater lengths, the rotational angle of the loaded edge would increase.

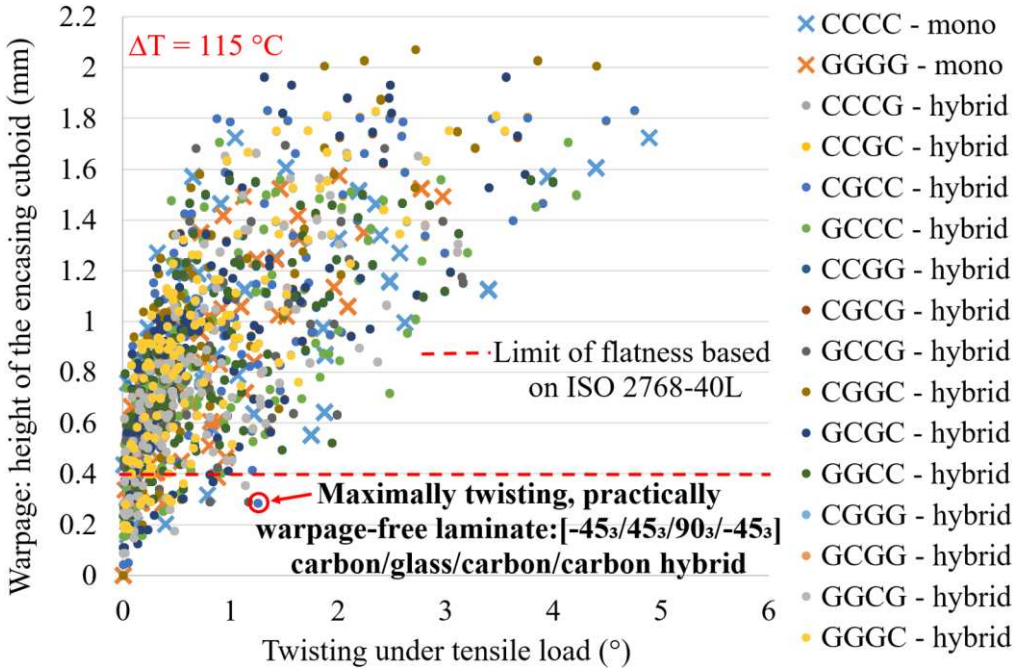

Figure 5 Numerical results for the 40 mm x 40 mm 12-ply (4 x 3 plies) mono and hybrid laminates: warpage at ΔT=115 °C and twisting at 0.5% tensile strain, where C refers to carbon and G refers to glass reinforcement

Figure 6 illustrates the experimental (3D scanning) validation of the numerical thermal warpage results of the best-performing mono and hybrid laminates. The numerical results slightly underestimated the warpage of the carbon laminate and slightly overestimated the warpage of the glass laminate, but the simulated results were practically within the standard deviation range of the experimental results. The only significant difference between experimental and numerical results was in the case of the hybrid specimens. The hybrid laminate had a more significant thermal warpage in reality than what the simulations predicted, about 20% larger on average. Several factors may have contributed to this difference, such as slight manufacturing inaccuracies or getting closer to the bifurcation point, which changes the shape of the laminate slightly but is not always handled well by the numerical solver. Nevertheless, the tested warpage of the hybrid laminate remained well under the limit of flatness (0.4 mm, ISO 2768-40L).

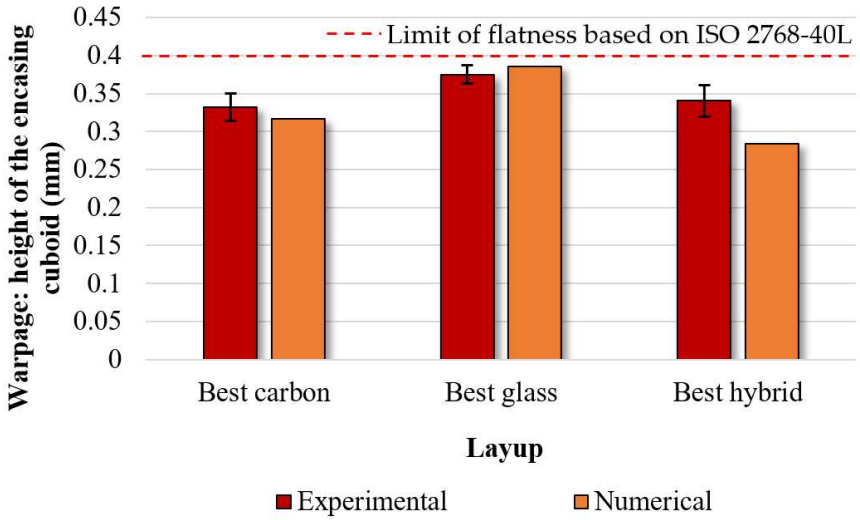

Figure 6 Thermal warpage results (ΔT=115 °C) of the 40 mm x 40 mm best carbon ([45_3 /-45_3 /45_3 /-45_3]), best glass ([45_3 /-45_3 /45_3 /90_3]) and best hybrid ([-45_3 /45_3 /90_3 /-45_3], carbon/glass/carbon/carbon) laminates based on the layup search study in Figure 5

Figure 7 illustrates the experimental extension–twist results in comparison with the numerical simulations. The coefficient of determination (R^2) of the fitted second-order polynomial trendlines was greater than 0.95 even for the most scattered datasets. At 0.5% tensile strain, the measured torsion of the loaded edge of the carbon laminate was 0.81° (±0.07°) (3.5% numerical underestimation, see Figure 7/a), 0.44° (±0.03°) for the glass laminate (98.5% numerical overestimation, see Figure 7/b) and 1.14° (±0.06°) for the hybrid layup (10.4% numerical overestimation, see Figure 7/c). The differences between the numerical and experimental results mainly resulted from the applied grip during the experiments. The grips prevented any transverse bending of the edges, unlike in the original simulations, where the loaded edge had free movement in directions other than the tensile direction. The restrictions at the loaded edge significantly changed the deformation pattern of the glass laminates but had a less pronounced effect on the carbon and the hybrid results. This is because the deflection of the corner points of the loaded edge (from which the global torsional angle is calculated) can not only result from twisting deformation but also from transverse bending. And in the case of the glass laminate, the majority of the deflections would result from transverse bending (because of the layup), unlike in the case of the carbon and the hybrid laminates. The original numerical model for the layup search study was put together to simulate a loading scenario where extension–twist laminates are most likely to be used: turbine or rotor blades. The tensile forces resulting from the rotation of the blades do not restrict out-of-plane movements such as transverse bending, so the simulations were run accordingly. To bridge the gap between the numerical and experimental results, we ran three additional simulations (one for each type of laminate), now modelling the steel grips (with bonded contact), too, and defining the fixed boundary condition on one of the grips and the in-plane displacement on the other grip, to accurately simulate the experiments. Figure 7 includes both the non-clamped (original) and the clamped (modified with grips) numerical results. As expected, in the case of the glass laminate, the clamped numerical simulations were in better agreement with the experimental results than the non-clamped numerical simulations (Figure 7/b). Clamping did not affect the hybrid results significantly but

slightly increased the twisting deformation of the carbon laminate due to the altered deformation pattern. In general, the clamped numerical results agreed well with the experiments, overestimating the average experimental results only by 18.2%, 5.8% and 11.1% for the carbon, glass and hybrid laminates, respectively. These differences may have been caused by accidental laminate pretensioning caused by the clamping and some mechanical resistance of the "freely rotating" grips. In summary, the best hybrid layup outperformed the best mono layup by 43.5% based on the original (non-clamped) numerical simulations, by 32.6% based on the modified (clamped) numerical simulations and by 40.7% based on the experimental results in terms of the extension–twist performance.

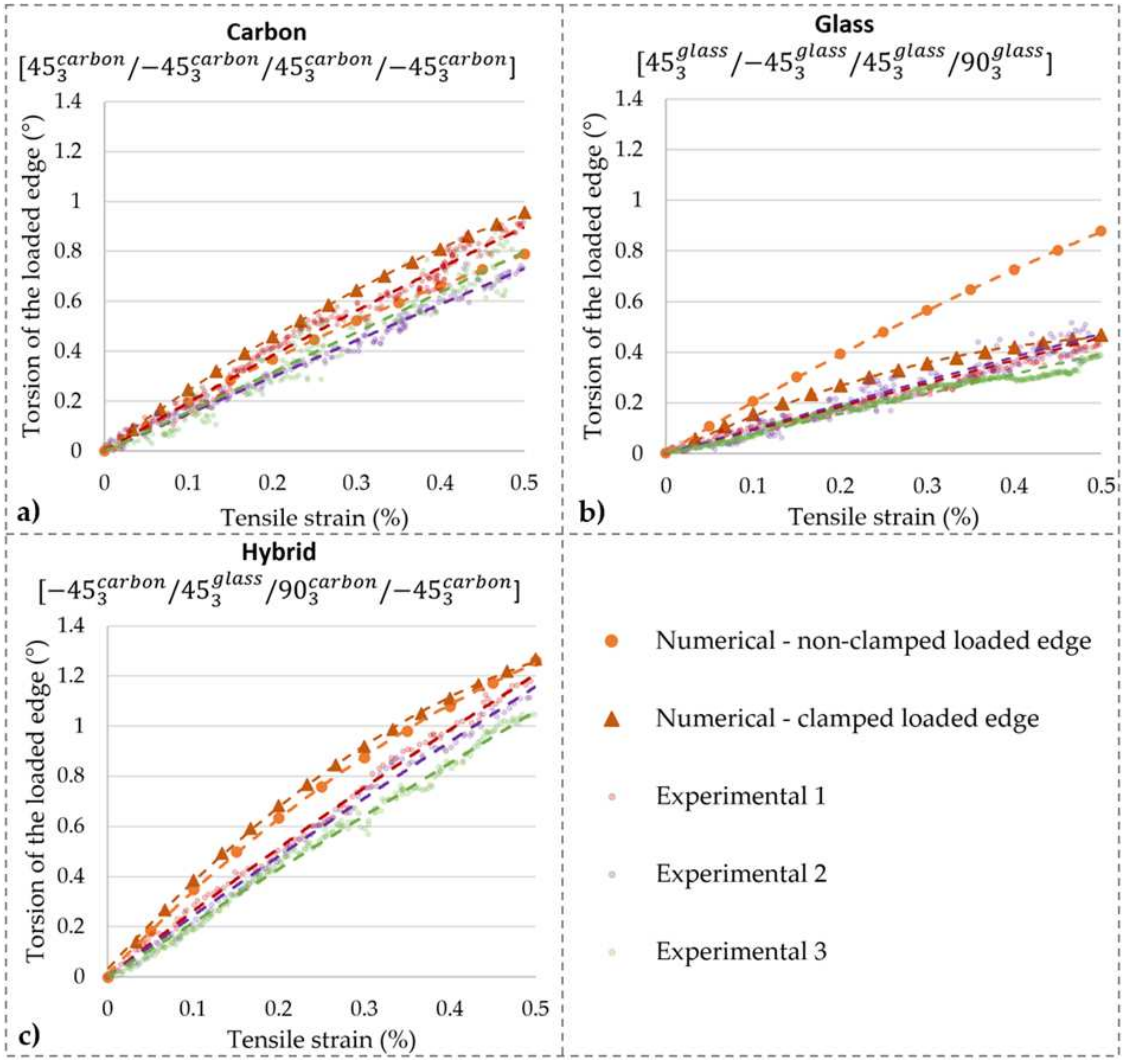

Figure 7 Numerical and experimental results of the best a) carbon, b) glass and c) hybrid extension–twist laminates based on the layup search study shown in Figure 5

4. Conclusions

We analyzed the thermal warpage, the bend–twist and the extension–twist behaviour of hybrid and non-hybrid monostable laminates through analytical, numerical and experimental investigations. The results proved that layup hybridization can significantly improve the extension–twist performance of practically warpage-free laminates (more than 30% improvement compared to mono laminates). Or from another

perspective, we showed that at a given extension–twist performance, where mono laminates would demonstrate significant thermal warpage, layup hybridization can keep the laminate practically warpage-free. In this regard, layup hybridization is an effective way to mitigate the warpage of extension–twist coupled composites. The bend–twist performance did not benefit from the hybridization mainly because this type of coupled behaviour does not require layup asymmetry and therefore, the warpage-mitigating capability of layup hybridization could not be fully exploited.

The main industrial value of the results is the improved achievable extension–twist performance of shape-adaptive structures without the disadvantage of significant thermal warpage, which pushes the limits of real-world applicability of advanced coupled composites.

Declaration of conflict of interests

The author(s) declared no potential conflicts of interest with respect to the research, authorship, and/or publication of this article.

Funding

The research reported in this paper is part of project no. BME-NVA-02, implemented with the support provided by the Ministry of Innovation and Technology of Hungary from the National Research, Development and Innovation Fund, financed under the TKP2021 funding scheme. The project was also funded by the National Research, Development and Innovation (NKFIH) Fund (project title: Development of multi-purpose fixed-wing drone based on innovative solutions and the creation of necessary competencies; ID number: 2019-1.1.1-PIACI-KFI-2019-00139). Furthermore, the research was supported by the ÚNKP-21-3 New National Excellence Program of the Ministry of Human Capacities.

References

1. Kessler MR, Sottos NR, White SR. Self-healing structural composite materials. *Compos Part A Appl Sci Manuf* 2003; 34: 743–753. DOI: 10.1016/S1359-835X(03)00138-6.
2. Wang Q, Meng J, Ma Y, et al. Thermally assisted self-healing and shape memory behaviour of natural rubber based composites. *Express Polym Lett* 2021; 15: 929–939. DOI: 10.3144/expresspolymlett.2021.75.
3. Chen F, Xiao H, Peng ZQ, et al. Thermally conductive glass fiber reinforced epoxy composites with intrinsic self-healing capability. *Adv Compos Hybrid Mater* 2021; 4: 1048–1058. DOI: 10.1007/s42114-021-00303-3.
4. Forintos N, Czigány T. Reinforcing carbon fibers as sensors: The effect of temperature and humidity. *Compos Part A Appl Sci Manuf* 2020; 131: 105819. DOI: 10.1016/j.compositesa.2020.105819.
5. Ashir M, Cherif C. Development of shape memory alloy-based adaptive fiber-reinforced plastics by means of open reed weaving technology. *J Reinf Plast Compos* 2020; 39: 563–571.
6. Motley MR, Liu Z, Young YL. Utilizing fluid–structure interactions to improve energy efficiency of composite marine propellers in spatially varying wake. *Compos Struct* 2009; 90: 304–313. DOI: 10.1016/j.compstruct.2009.03.011.
7. Shakya P, Sunny MR, Maiti DK. A parametric study of flutter behavior of a composite wind turbine blade with bend-twist coupling. *Compos Struct* 2019; 207: 764–775. DOI:

10.1016/j.compstruct.2018.09.064.

8. York CB. Extension-twist coupled laminates for aero-elastic compliant blade design. In: *53rd AIAA/ASME/ASCE/AHS/ASC Structures, Structural Dynamics and Materials Conference*. Honolulu, 2012, p. AIAA-2012-1457. DOI: 10.2514/6.2012-1457.
9. Cross RJ, Haynes RA, Armanios EA. Families of hygrothermally stable asymmetric laminated composites. *J Compos Mater* 2008; 42: 697–716. DOI: 10.1177/0021998308088597.
10. Hyer MW. Some Observations on the Cured Shape of Thin Unsymmetric Laminates. *J Compos Mater* 1981; 15: 175–194. DOI: 10.1177/002199838101500207.
11. Hyer M. The room-temperature shapes of four-layer unsymmetric cross-ply laminates. *J Compos Mater* 1982; 16: 318–340. DOI: 10.1177/002199838201600406.
12. Baran I, Cinar K, Ersoy N, et al. A review on the mechanical modeling of composite manufacturing processes. *Arch Comput Methods Eng* 2017; 24: 365–395. DOI: 10.1007/s11831-016-9167-2.
13. Kappel E. Compensating process-induced distortions of composite structures: A short communication. *Compos Struct* 2018; 192: 67–71. DOI: 10.1016/j.compstruct.2018.02.059.
14. Tsai SW, Melo JDD. *Composite materials design and testing - unlocking mystery with invariants*. Stanford: Composites Design Group, 2015.
15. Haynes RA. New families of hygrothermally stable composite laminates with optimal extension-twist coupling. *AIAA J* 2010; 48: 2954–2961. DOI: 10.2514/1.J050596.
16. Li J, Li D. Multi-objective optimization of hygro-thermally curvature-stable antisymmetric laminates with extension-twist coupling. *J Mech Sci Technol* 2014; 28: 1373–1380. DOI: 10.1007/s12206-013-1171-y.
17. Kollár LP, Springer GS. *Mechanics of composite structures*. Cambridge: Cambridge University Press, 2003.
18. Czél G, Wisnom MR. Demonstration of pseudo-ductility in high performance glass/epoxy composites by hybridisation with thin-ply carbon prepreg. *Compos Part A Appl Sci Manuf* 2013; 52: 23–30. DOI: 10.1016/j.compositesa.2013.04.006.
19. Kim JJ, Brown AD, Bakis CE, et al. Hybrid carbon nanotube - carbon fiber composites for high damping. *Compos Sci Technol* 2021; 207: 108712. DOI: 10.1016/j.compscitech.2021.108712.
20. Pattar N, Patil SF. Review on fabrication and mechanical characterization of shape memory alloy hybrid composites. *Adv Compos Hybrid Mater* 2019; 2: 571–585. DOI: 10.1007/s42114-019-00119-2.
21. Rev T, Jalalvand M, Fuller J, et al. A simple and robust approach for visual overload indication - UD thin-ply hybrid composite sensors. *Compos Part A Appl Sci Manuf* 2019; 121: 376–385. DOI: 10.1016/j.compositesa.2019.03.005.
22. Daynes S, Weaver P. Analysis of unsymmetric CFRP–metal hybrid laminates for use in adaptive structures. *Compos Part A Appl Sci Manuf* 2010; 41: 1712–1718. DOI: 10.1016/j.compositesa.2010.08.009.
23. HexTow IM7 carbon fiber - product data sheet. Hexcel Corporation, https://www.hexcel.com/user_area/content_media/raw/IM7_HexTow_DataSheet.pdf (2020).

24. HexPly 913 125°C curing epoxy matrix - product data sheet. Hexcel Corporation, https://www.hexcel.com/user_area/content_media/raw/HexPly_913_eu_DataSheet.pdf (2020).
25. Barbero EJ. *Introduction to composite materials design*. 3rd ed. Boca Raton: Taylor & Francis Group, 2018.